Electronic Supplementary Material (ESI) for Journal of Materials Chemistry B.


# Supporting Information

# Poly(succinimide) Nanoparticles as Reservoirs for Spontaneous and Sustained Synthesis of Poly(aspartic acid) under Physiological Conditions: Potential for Vascular Calcification Therapy and Oral Drug Delivery

Hossein Adelnia[1,2,4], Idriss Blakey[1,5], Peter J. Little[4], Hang T. Ta[1,2,3],*

[1]Australian Institute for Bioengineering and Nanotechnology, University of Queensland, Brisbane, 4067, Queensland, Australia

[2]Queensland Micro- and Nanotechnology Centre, Griffith University, Brisbane, 4111, Queensland, Australia

[3]School of Environment and Science, Griffith University, Brisbane, 4111, Queensland, Australia

[4]School of Pharmacy, the University of Queensland, Brisbane, 4102, Queensland, Australia

[5]Centre for Advanced Imaging, University of Queensland, Brisbane, 4067, Queensland, Australia

*Correspondence to Hang T. Ta; Email: h.ta@griffith.edu.au

## Characterization of PSI and PASP

FTIR spectra of aspartic acid monomer, PSI and PASP are shown in Fig. S1. The characteristic peaks of PSI are seen at 1394, 1708 and 3382 $cm^{-1}$, while those of PASP are at 1395, 1557, and 3270 $cm^{-1}$. The characteristic peaks of PSI have been reported to be at 1795 (weak as a shoulder), 1713 (sharp), 1391, and 1361 (together relatively sharp), and 3362 (broad) (1). The absorption bands at 1713 $cm^{-1}$ and 1795 $cm^{-1}$ were attributed to the coupled effect of two neighboring carbonyl groups, showing the structure of imide rings which is further proved by their disappearance after ring opening via hydrolysis (2). The band at 3382 $cm^{-1}$ is attributed to stretching vibration of NH band in PSI. For PASP however, the characteristic peaks are usually observed at wavelength values around 3280 (broad), 1560 (sharp and relatively broad), 1390 (sharp), 1620 (shoulder) (3, 4). In accordance with the spectra obtained by Zhang et al. and Gao et al. (3, 4), PASP synthesized in this study showed the same characteristic peaks. It should be noted that possibly due to different degree of neutralization, presence of counter-ion, and different position of carboxylic acid group (i.e., α, or β) in PASP, the characteristic peaks of PASP in the literature are to some extent different. However, the overall pattern is similar (2-6).

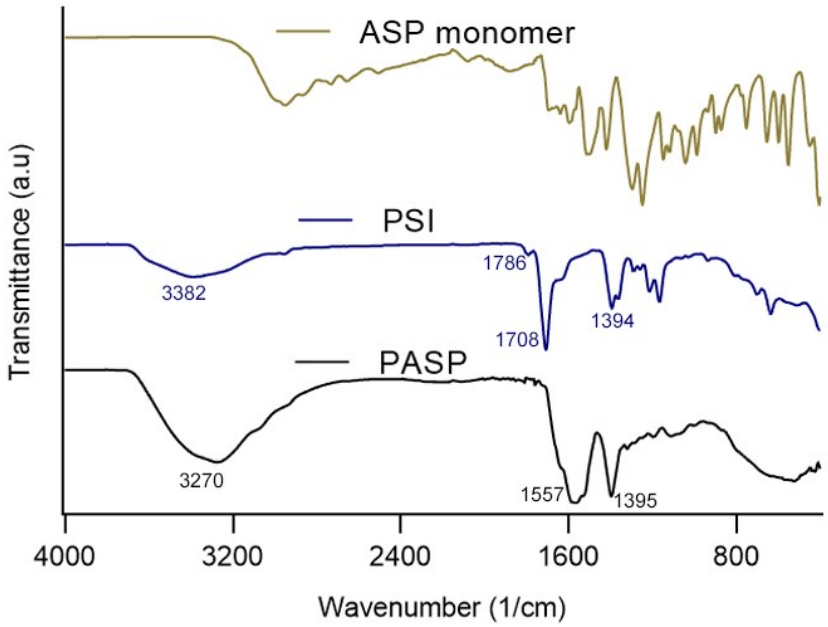


**Fig. S1.** FTIR spectra of aspartic acid monomer, PSI and PASP.

Regarding the H-NMR of PSI in d6-DMSO, the characteristic peaks are at 2.7, 3.21, and 5.28 ppm (Fig. S2). The first two peaks with approximately similar intensities and area under curve values are related to methylene proton, while the last one is attributed to methine proton. Water molecules as impurity show peak at 3.33 ppm overlapping with the 3.21 ppm peak of methylene proton. The band at around 2.5 is attributed to DMSO (7). The synthesized polymer showed relatively high molecular weight. The fitted molecular weight based on polyethylene glycol standard curve was $M_w$=84.8 kDa, $M_n$=66.7 kDa, and Đ =1.27.

Thermal stability of the papered polymers was also evaluated (Fig. S3). The TGA and DTG (the first derivative of the TGA curve) traces of the polymers are consistent with those reported in the literature (8, 9). PSI was found to have a 2-stage degradation and to be more stable than Na-PASP specifically at temperatures lower than 300 °C. The final weight at 600 °C for PSI and Na-PASP are respectively 0 and 24%. The relatively high weight at this temperature for Na-PASP is due to sodium ions that are not evaporated as degradation product/gas. Considering

the molar mass of sodium ions (22.99 g/mol) vs. aspartic acid repeating unit (115 g/mol), the weight ratio of sodium to sodium salt of aspartic acid is 0.166 which is close to the final weight of Na-PASP at 600 °C in TGA curve (i.e., 24%), implying the absence of impurity in the sample.

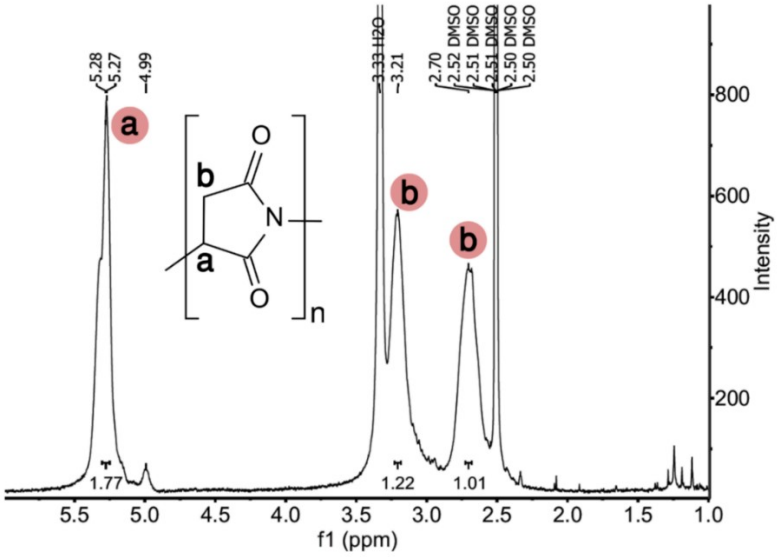


**Fig. S2.** H-NMR spectrum of PSI in d6-DMSO synthesized by poly-condensation reaction of aspartic acid at 180 °C for 5 hours.

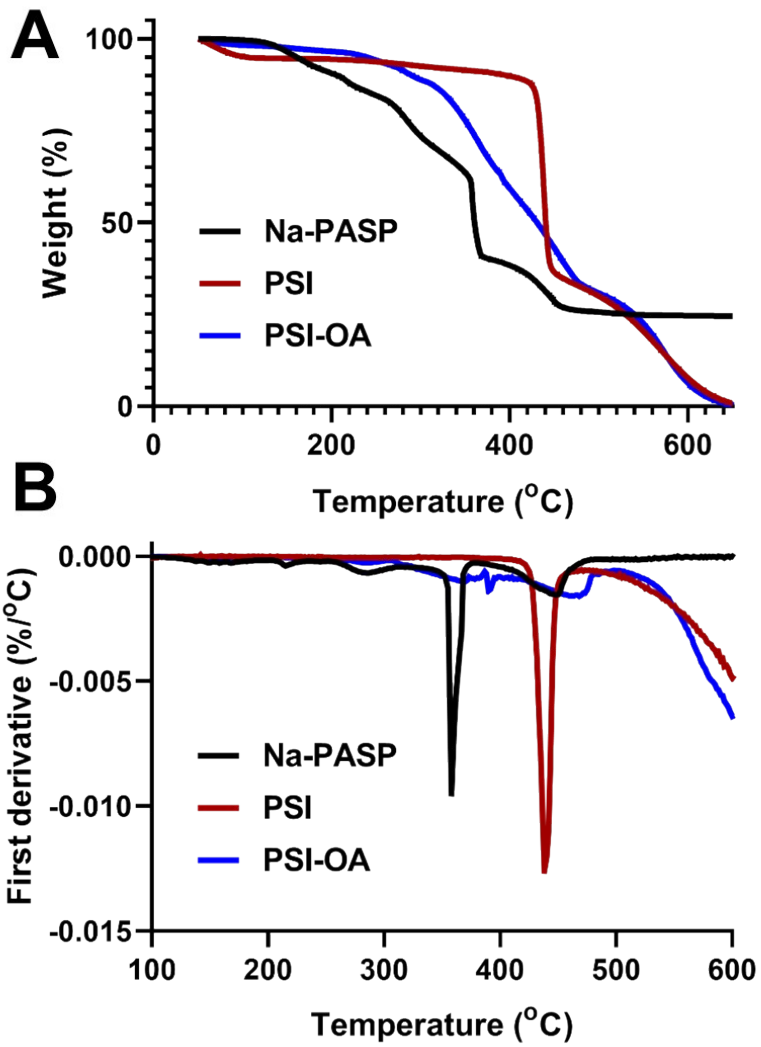


**Fig. S3.** Thermal properties of the resulting polymers (A) TGA, (B) first derivative of TGA.

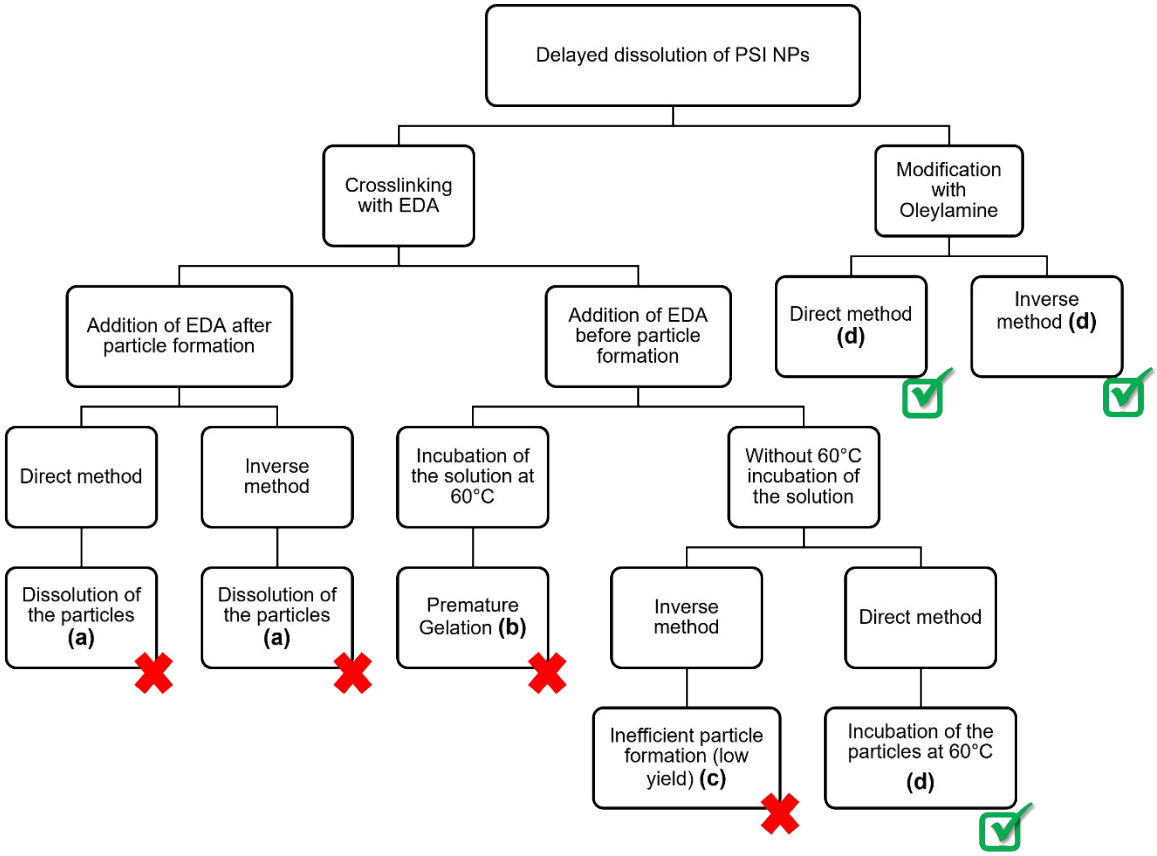


**Fig. S4**. Use of various approaches to delay and prolong the dissolution of PSI NPs. **(a)** EDA reaction at particle surface with succinimide units led to particle size decrement, while at high concentration, complete solubilization of the particles was seen. **(b)** Incubation solution of PSI-EDA mixture accelerates the reaction and leads to premature gelation of the solution**. (c)** Due to low polymer concentration used in the inverse method (<0.625 wt.% resulted in low size with uniform distribution), the particle formation was inefficient when EDA was added. **(d)** Modification of the polymer with oleylamine as well as incubation of the particles at 60 ˚C led to delayed dissolution

Regarding the delayed dissolution of the PSI NPs, various approaches were tested as summarized in Fig. S4. The delayed dissolution by EDA crosslinking was only feasible in the direct method. This was achieved when EDA was added right before particle formation, followed by incubation of the particles at 60 °C for 4 h. The optimum concentration of the particles for incubation was 5 mg/mL, as higher concentration led to aggregation and particle size increment.

It should be noted that the addition of EDA after particle formation (in both direct and inverse methods) led to size decrement at low concentration (<2.5 mol% of EDA) and complete solubilization of the particles at high concentration (>7.5 mol% of EDA). The application of more hydrophobic cross-linkers such as hexamethylenediamine, or 1,12-diaminododecane were not effective either. The incubation (60 °C) of PSI-EDA solution (in DMSO) accelerated the crosslinking reaction and led to the premature gelation, thereby making the nano-precipitation impossible. The gelation time was dependent upon the EDA concentration varying from approximately 5 to 30 min for 10, and 2.5 mol.%, respectively. Furthermore, for the modification of PSI with oleylamine, regardless of the method used (direct or inverse), the

particles were stable and almost similar dissolution profile was observed for the direct and inverse method.

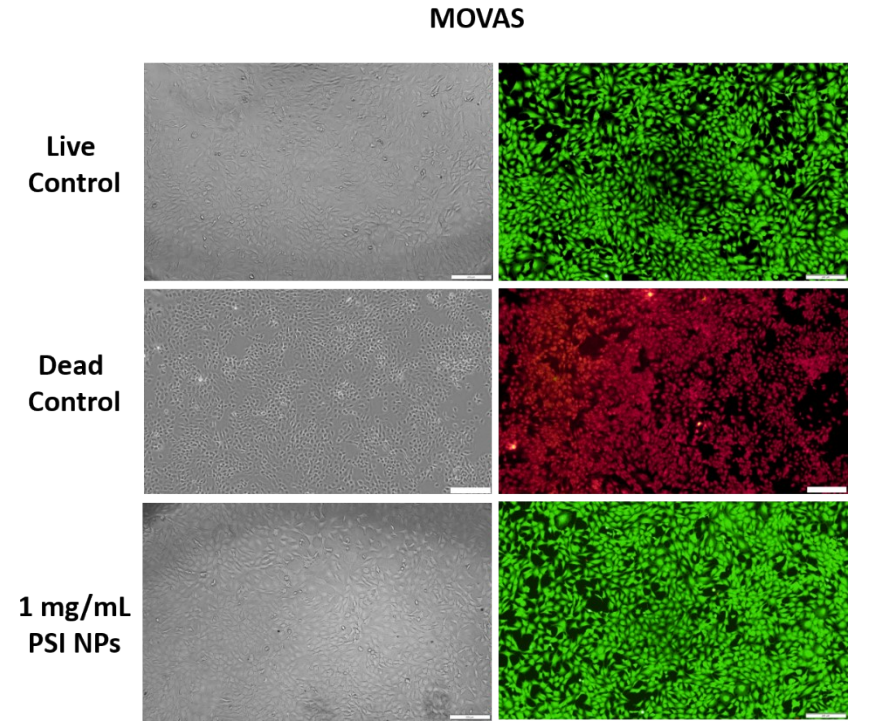


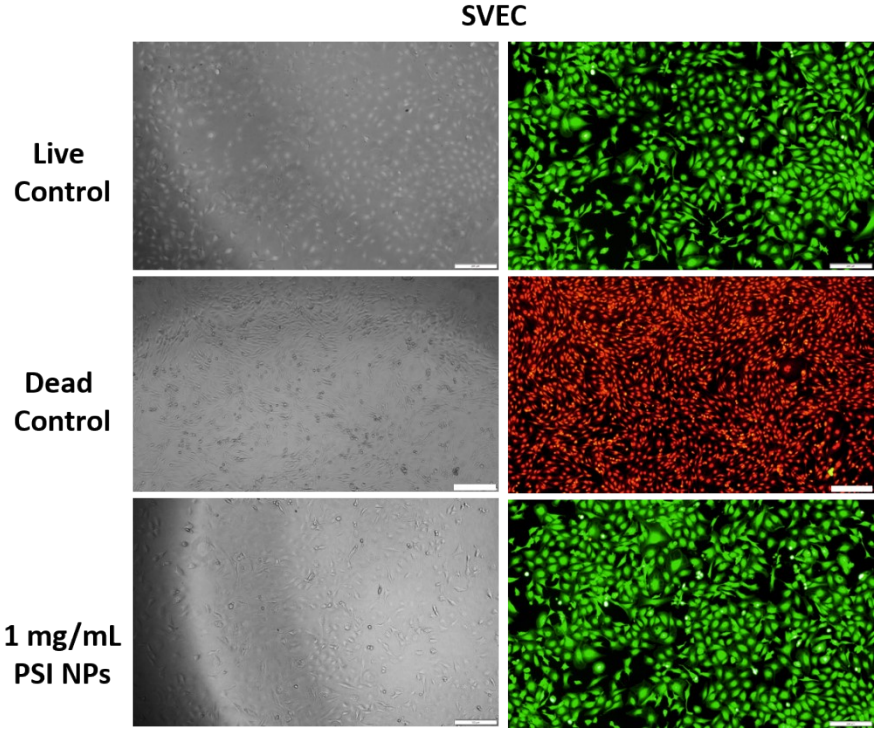

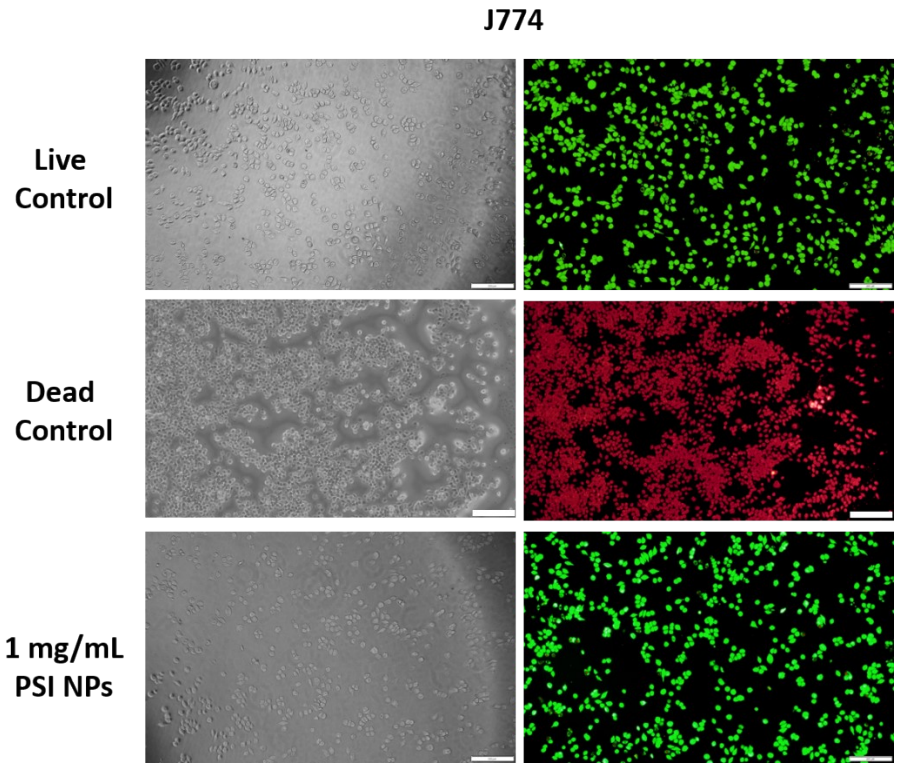


**Fig. S5.** Optical microscopic images of MOVAS, SVEC, and J774 (brightfield and fluorescence, respectively on the left and right) treated with growth medium (live control), 30% of methanol (dead control), and 1 mg/mL of the NPs. The scale bars in all images are 200 µm.

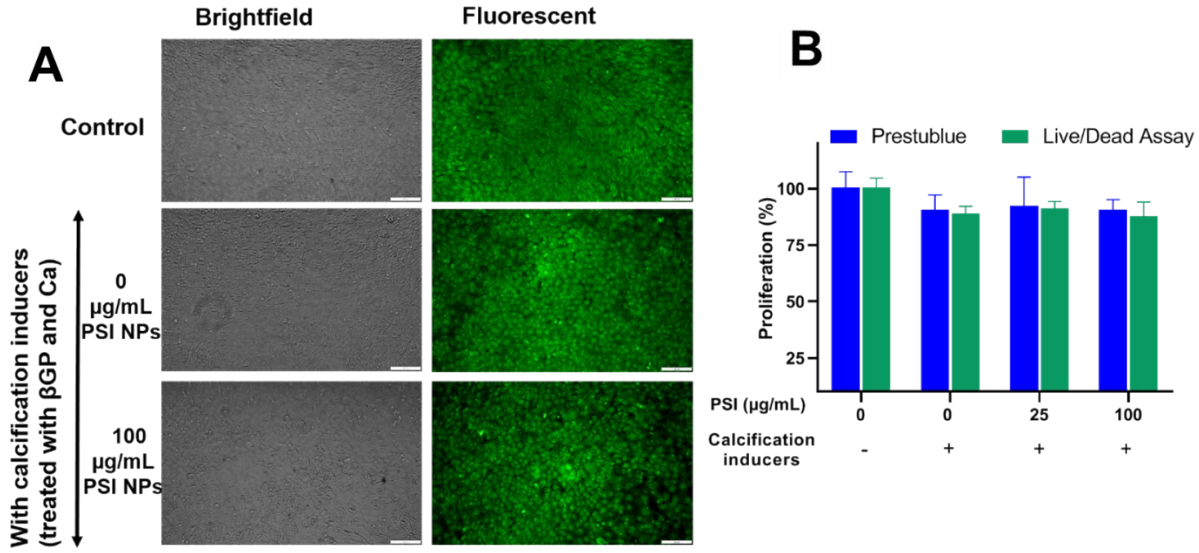


**Fig. S6. Viability of MOVAS after 12 days of treatment with the calcification inducers (with and without PSI NPs).** The medium was refreshed every 3 days. The scale bar is 50 µm. Data are presented as mean ± SD of at least 6 replicates for Prestoblue assay. The treatment group was normalized to the live control (i.e., no calcification inducer).

**Table S1**. Size and zeta potential of the PSI NPs prepared by inverse and direct precipitation method.

| **Direct Method** | | | | **Inverse method** | | | |
|---|---|---|---|---|---|---|---|
| **PSI concentration (wt.%)** | Size (nm) | PDI | Zeta potential (mV) ** | **PSI concentration (wt.%)** | Size (nm) | PDI | Zeta potential (mV)** |
| **2.5** | 97 | 0.19 | -27.5 | **0.375** | 106 | 0.06 | -25.3 |
| **5** | 118 | 0.19 | -27.9 | **0.625** | 131 | 0.06 | -26.3 |
| **7.5** | 151 | 0.15 | -26.7 | **1.25** | 176 | 0.02 | -25.8 |
| **10** | 175 | 0.10 | -28.1 | **2.5%** | 267 | 0.19 | -24.9 |
| **12.5** | 196 | 0.28 | -25.5 | **5%** | 636 | 0.16 | -25.4 |
| **15*** | n.d | n.d. | n.d | **10%*** | 397 | 0.27 | -25.6 |

* Severe coagulation occurred.
**Zeta Potential values were measured at pH: 7.4.

**Table S2.** Z-average and zeta potential values of the PSI-NPs prepared by inverse nano-precipitation method in absolute ethanol at different PSI concentration

| PSI Conc. (wt.%) | Size (nm) | PDI |
|---|---|---|
| 0.375 | 195 | 0.08 |
| 0.625 | 255 | 0.06 |
| 1.25 | Severe coagulation | Severe coagulation |

**Table S3.** Z-average and zeta potential values of the PSI-NPs prepared by inverse nano-precipitation method. Different contents of ethanol were added to water to tune size and to assess stability. PSI concentration is constant at 1.25 wt.%.

| EtOH (vol.%) | Size (nm) | PDI |
|---|---|---|
| 0 | 176 | 0.02 |
| 60 | 203 | 0.67 |
| 80 | 263 | 0.13 |
| 100 | Severe coagulation | Severe coagulation |

## References:


1. Migahed M, Rashwan S, Kamel M, Habib R. Synthesis, characterization of polyaspartic acid-glycine adduct and evaluation of their performance as scale and corrosion inhibitor in desalination water plants. Journal of Molecular Liquids. 2016;224:849-58.
2. Zhang C, Wu S, Qin XJML. Facile fabrication of novel pH-sensitive poly (aspartic acid) hydrogel by crosslinking nanofibers. 2014;132:393-6.
3. Zhang C, Wan LY, Wu S, Wu D, Qin X, Ko FJD, et al. A reversible colorimetric chemosensor for naked-eye detection of copper ions using poly (aspartic acid) nanofibrous hydrogel. 2015;123:380-5.
4. Gao Y, Fan L, Ward L, Liu ZJD. Synthesis of polyaspartic acid derivative and evaluation of its corrosion and scale inhibition performance in seawater utilization. 2015;365:220-6.
5. Lim SL, Tang WNH, Ooi CW, Chan ES, Tey BTJJoAPS. Rapid swelling and deswelling of semi-interpenetrating network poly (acrylic acid)/poly (aspartic acid) hydrogels prepared by freezing polymerization. 2016;133(24).
6. Liu C, Chen Y, Chen JJCP. Synthesis and characteristics of pH-sensitive semi-interpenetrating polymer network hydrogels based on konjac glucomannan and poly (aspartic acid) for in vitro drug delivery. 2010;79(3):500-6.
7. Wolk SK, Swift G, Paik YH, Yocom KM, Smith RL, Simon ES. One-and two-dimensional nuclear magnetic resonance characterization of poly (aspartic acid) prepared by thermal polymerization of L-aspartic acid. Macromolecules. 1994;27(26):7613-20.
8. Adelnia H, Tran HD, Little PJ, Blakey I, Ta HT. Poly (aspartic acid) in Biomedical Applications: From Polymerization, Modification, Properties, Degradation, and Biocompatibility to Applications. ACS Biomaterials Science & Engineering. 2021.
9. Tudorachi N, Chiriac AP. TGA/FTIR/MS study on thermal decomposition of poly (succinimide) and sodium poly (aspartate). Polymer Testing. 2011;30(4):397-407.